

Sediment Dispersal and Provenance Analysis of the Upper Clair Group, Clair Field, West of Shetland Basin: Implications for Reservoir Architecture

Okechukwu Okpobiri^{1*}, Edirin Akpofure², Oborie Ebiegeri²

¹Department of Geology, Rivers State University, Nigeria. 500001

²Department of Geology, Niger Delta University, Nigeria.

Email address: Okechukwu.okpobiri@ust.edu.ng, edirinakpofure@yahoo.com, ebi.oborie@ndu.edu.ng

Abstract—The Clair Field is a significant oil and gas accumulation in the West of Shetland Basin, formed in response to the Caledonian orogeny. The basin's complex deformation history has resulted in highly fractured Devonian-Carboniferous reservoirs. Initial production challenges were attributed to reservoir heterogeneity and the intricate fracture/fault network. This study employs paleotransport analysis to reconstruct sediment dispersal patterns for the individual reservoirs of the Upper Clair Group. Dipmeter and borehole image log data from 32 wells ranging from vertical to horizontal and high-angled were analyzed using Task Geomodelling Attitude software. Structural tilt corrections and borehole bias adjustments were applied to derive azimuth vector mean, which were plotted on a base map. The Spheristat software was used to determine average spatial azimuth trends, while paleocurrent directions were calculated using Busk's circular arc method. The results indicate multiple sediment sources for individual reservoir units, with sediment dispersal patterns influenced by both tectonic and climatic factors. These findings have significant implications for understanding reservoir distribution and quality, which are crucial for hydrocarbon development and production.

Keywords— Clair Field, Paleotransport Analysis, Sediment Dispersal, Reservoir Architecture, Provenance, Hydrocarbon Production.

I. INTRODUCTION

The Clair Field, located in the West of Shetland Basin (WOSB), is the largest hydrocarbon discovery on the UK Continental Shelf (UKCS). Spanning license blocks 206/7, 206/8, 206/9, 206/12, and 206/15, it covers an area of 220 km², with estimated in-place reserves exceeding 7 billion barrels of oil (BP, 2021). The field comprises Devonian-Carboniferous sandstone reservoirs of the Clair Group, deposited in fluvial, lacustrine, shallow marine, and aeolian environments. Despite its resource potential, exploration and production in the Clair Field have been hindered by complex geology, including highly fractured reservoirs, variable sediment dispersal patterns, and challenging offshore conditions (Johnston et al., 1995a; Morton & Milne, 2012).

Sediment dispersal and paleocurrent analysis play a critical role in understanding the internal architecture of a reservoir. The movement of sediments within a basin is controlled by a combination of tectonics, climate, provenance, and depositional processes (Dickinson, 1988). In fluvial and shallow marine systems, paleocurrent data—derived from cross-bedding, ripple marks, and imbricated clasts—provide

insights into the direction of sediment transport and the spatial distribution of reservoir-quality sandstones (Boggs, 2011).

In the oil and gas industry, paleotransport analysis helps predict the location of high-permeability sand bodies versus low-permeability mudstones, which influence reservoir heterogeneity and connectivity (Nichols, 2005). This understanding enhances reservoir modelling and production strategies (Morton & Milne, 2012). In complex geological settings, such as the Clair Field, sediment dispersal is influenced by fault-controlled drainage systems, fluctuating water levels, and multi-source contributions (Schmidt et al., 2013). Identifying these patterns is essential for optimizing well placement, water flood strategies, and enhanced oil recovery (EOR) techniques. This study employs paleotransport analysis using borehole image logs and dipmeter data to refine sediment dispersal models in the Clair Field, providing new insights into reservoir architecture and hydrocarbon recovery potential.

II. THE STUDY AREA

The West of Shetland Basin (WOSB) is a structurally complex sedimentary basin that evolved through multiple phases of tectonic activity from the Devonian to the Cretaceous. The basin's formation is closely tied to the Caledonian orogeny, which shaped the North Atlantic region and provided the structural framework for subsequent sediment deposition (Schmidt et al., 2013). The WOSB is bounded by major fault systems, including the NE-SW trending Shetland Spine Fault to the southeast and the Rona Ridge to the northwest, forming a horst-and-graben structural configuration (Allen & Mange-Rajetzky, 1992) (see Figure 1).

The Clair Field, situated within the WOSB, contains reservoir sandstones that reflect a dynamic environment influenced by tectonic subsidence and climatic variations (Nichols, 2005). Initially, the WOSB functioned as an endorheic basin, with internally draining river systems depositing sediments from surrounding highlands, including potential sources in Scandinavia, East Greenland, and Scotland (Morton & Milne, 2012).

By the Mesozoic, the basin experienced periods of subsidence and uplift due to regional extensional tectonics associated with the opening of the North Atlantic. While much of the surrounding region underwent significant marine

transgressions, the Clair Field remained dominated by continental sedimentation, with overlying Cretaceous Shetland Group shales acting as a regional seal (Johnston et al., 1995a). The interplay of faulting and differential subsidence during this period further compartmentalized the reservoir, contributing to its present-day complexity.

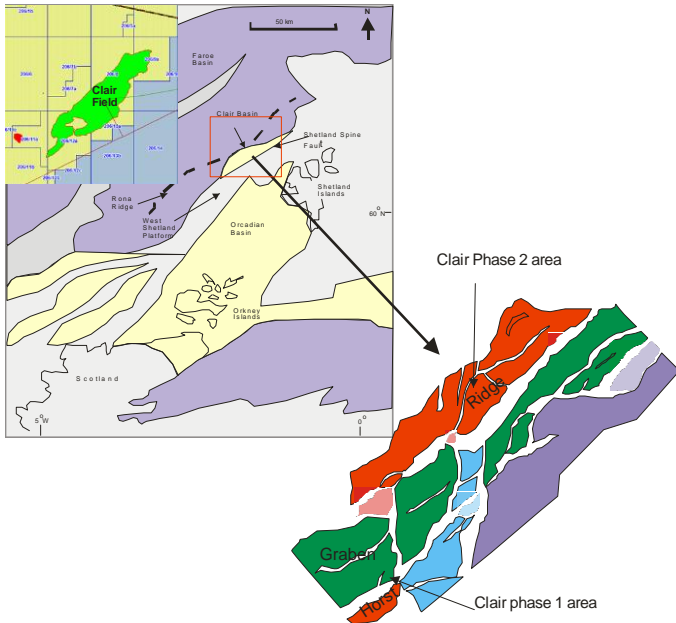


Figure 1. Structure of the Clair Field spanning 5 license blocks and the location of the ridge, graben and horst and the development phase targets (after Clair fracture study TSK-09-37).

Stratigraphy	Lithology	Depositional Environment	Thickness	Mineral Composition
Cretaceous Shetland Group Shale				
Carboniferous	Unit X	Marginal marine	Variable	Garnet, Zircon, Epidote, Rutile, Staurolite, Titanite, Apatite, Tourmaline
	Unit IX	Fluvial system	Variable	Garnet, Zircon, Epidote, Rutile, Staurolite, Titanite, Apatite, Tourmaline
	Unit VIII	Fluvial system	Variable	Garnet, Epidote, Zircon, Titanite, Rutile, Staurolite, Apatite, Tourmaline
Devonian	Upper unit VI	Fluvial/Lacustrine	135 - 190	Garnet, Zircon, Rutile, Staurolite, Apatite, Tourmaline
	Lower unit VI	Lacustrine		
	Unit V	Fluvial/Lacustrine	93 - 106	Apatite, Garnet, Tourmaline, Zircon
	Unit IV	Fluvial channel		
	Unit III	Fluvial sands with aeolian reworking	103 - 170	Apatite, Garnet, Tourmaline, Zircon
	Unit II	Fluvial system		
Unit I	Fluvial - lacustrine fan delta	19 - 66	Garnet, Zircon, Rutile, Staurolite, Apatite, Tourmaline	
	Lacustrine Fan delta	12 - 194	Unstable minerals	
Metamorphic Gneiss				

Figure 2: Stratigraphy of the Clair Group units I – IX (after Nichols, 2005)

The Cenozoic era saw significant uplift and erosion across the WOSB due to renewed tectonic activity linked to the Icelandic Plume and the final rifting of the North Atlantic (Fletcher et al., 2013). These geological events altered burial depths, influencing hydrocarbon generation, migration, and trapping within the Clair reservoirs. The fractured nature of the Devonian-Carboniferous sandstones, coupled with long-term structural reactivation, played a key role in reservoir heterogeneity and fluid flow behaviour (Stoker et al., 2017).

III. MATERIALS AND METHODS

Data Set

A plethora of image logs have been used and they all have different resolutions see Table 1. The data set used in this study are digitized and manually oriented picks interpreted from multiple borehole image logs by different companies. It includes the following:

- Thirty-two wells, five of which are confidential and therefore unavailable (Appendix 1a). Figure 3 shows their spatial orientation.
- Stratigraphy and formation tops.
- Directional surveys, position logs and borehole deviation data for wells.

TABLE 1: Image tools used in the Clair Field and their intrinsic quality.

Image log	Image Type	Quality
Core Image	Goniometry	Excellent
Fullbore Formation Microimager (FMI)	Wireline	Good - excellent
StarTrak	Wireline	Moderate to good
Azimuthal Litho Density (ALD) /Azimuthal Neutron Density (AND)	LWD	Moderate to good
Oil Based Microimager (OBMI)	Wireline	Poor to good
Ultrasonic Borehole Imager (UBI)	Wireline	Poor to good
OnTrak (azimuthal gamma-ray)	LWD	Poor to moderate
Circumferential Borehole Imaging Tool (CBIL)	Wireline	Poor to moderate
LithoTrak (azimuthal density LWD)	LWD	Poor to moderate

Data normalization

Data standardization necessary for collating data from different wells and sources was done using the Task Geoscience standardized classification scheme (Appendix 1b). Although this study doesn't focus on fractures and faults, they are also included to enhance interpretation by eliminating possible fault drag patterns. Unit IV has a good example of cross-stratified bedding dips which are identified by a cusped shape in the tadpole track. Beds might be pulled down during faulting (fault drag) resulting in cusps, but these are not because there is just one fracture dip (Figure 4).

averaging on local scale around the cluster and on large scale (Appendix 18-23). Paleoflow lines were derived using Busk's circular arc technique. Paleoflow on a large scale and on a local scale (for variance) were obtained (Figure 6). Finally, channel sinuosity was derived using circular arc method.

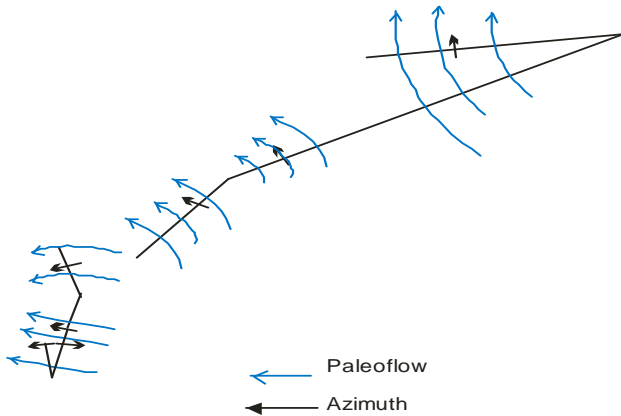


Figure 6: Deriving paleoflow using the Busk's circular arc method.

IV. RESULT AND DISCUSSION

Upper Unit VI

This Unit is dominated by sandstones. The rose diagram shows a predominant SW azimuth trend and a minor NW trend with local scatter (Figure 7). The large scale displays a unidirectional SW azimuth trend which scatters towards the cluster and then diverges into SE and SW orientations downstream. The sinuosity index is high north of the basin, increases within the cluster and reduces downstream. Locally within the cluster, is a bimodal SW and SE azimuth trend. The SE trend is unidirectional with variations increasing downstream accompanied by a low sinuosity. Whereas the SW trend show a minor NW orientation across the basin accompanied with increasing sinuosity downstream. (Appendix 20).

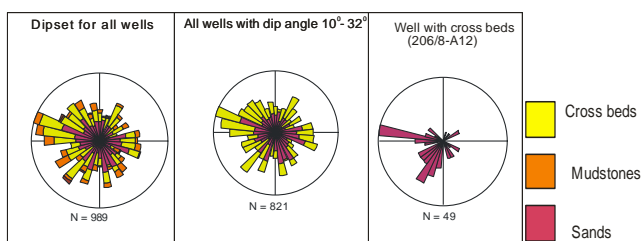


Figure 7: Paleotransport analysis result from interpreted lithofacies dip set for Upper Unit VI

Heavy mineral composition established by Schmidt *et al* (2013) and Morton (2012) consists of: type 2 zircon, low staurolite- zircon ratio (SZi), low rutile-zircon ratio (RuZi), high ATi and GZi increasing downhole (Schmidt *et al.*, 2013) (Figure 8) Paleogeographic model suggests a northern provenance (Nichols, 2005), see Figure 9. This unidirectional trend with spread typical of a fluvial system reflects a northern source, as suggested by the paleogeography but by an axial, not a transverse system. Flowing axial to the major fault signifies eroding sediments

off the alluvial plain, hence the dominant Manganese-garnet and type 2 zircon. The sinuosity value and palaeocurrent indicates a meandering river bifurcating downstream.

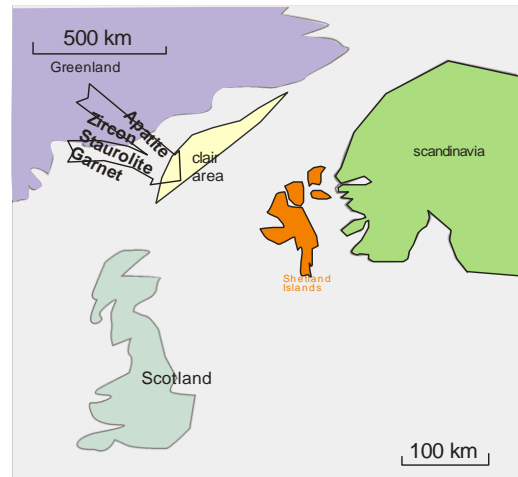


Figure 8: Provenance map based on heavy mineralogy. Sourcing is solely from the north (after Allen & Mange-Rajetzky, 1992)

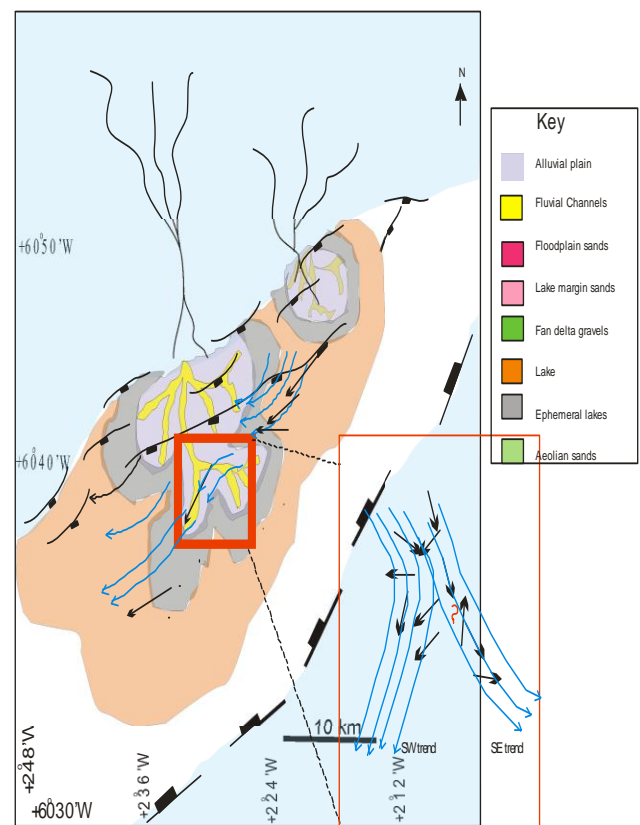


Figure 9: Paleoflow for upper unit VI plotted on the paleogeographic map indicating a northern provenance with local spread (after Nichols, 2005).

The meandering at bifurcation by the SW trend as implied by the high sinuosity value has an implication for "channel abandonment or enlargement periodically" (Kleinhaus *et al.*, 2011) (Figure 10).

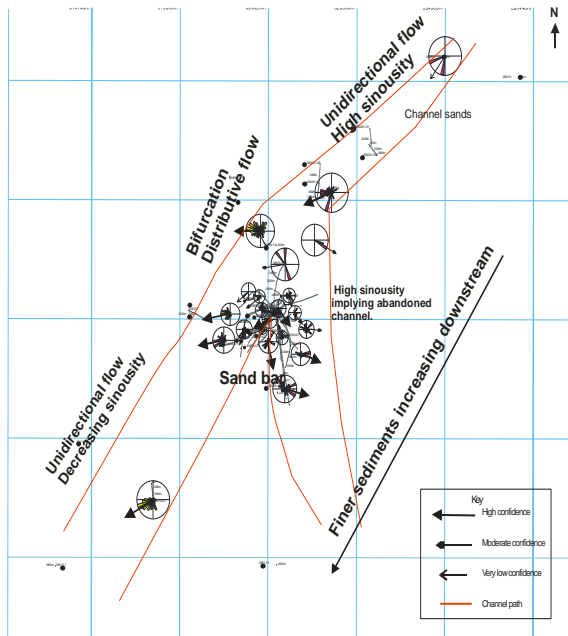


Figure 10. Base map showing the interpreted river course and the sandstone distribution as derived from the azimuth trends and sinuosity values.

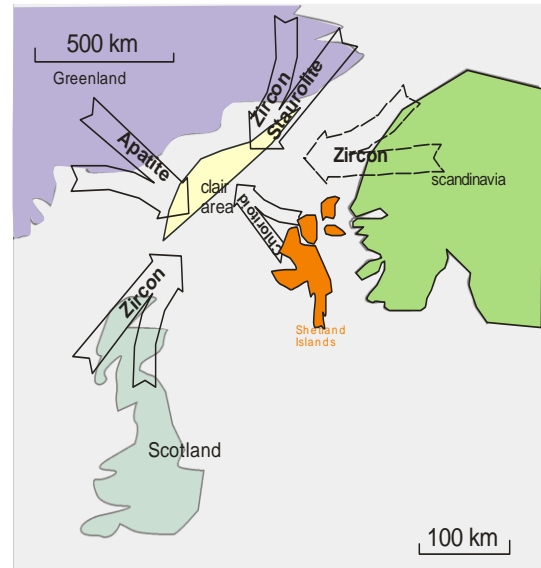


Figure 12: Provenance map showing confirmed sources in bold lines and likely sources in dashed lines showing an increase in drainage area (after Morton & Milne, 2012).

Unit VII/VIII

Unit VII/VIII is a sandstone rich interval. The rose diagram shows a bimodal orientation: a predominant SW trend and a minor NW trend with scatter (Figure 110). Basin wide, the dispersal pattern features a dominant SW orientation with scatter upstream, reducing downstream with variations in the SE directions. The sinuosity index is low upstream, increases at the cluster and reduces downstream only in the SE trend while the SW trend maintains a high sinuosity downstream. Revealed at the local scale is a predominant SE trend with scatter in the SW, NE and NW. The SE trend features a principal SE orientation with local variations: SW and NW. The SW trend is dominant with scatter in the SE direction. The NE and NW trend are unidirectional (Appendix 21).

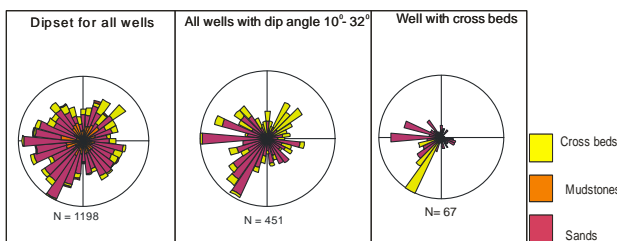


Figure 11: Paleotransport analysis result from interpreted lithofacies dip set for Unit VII/VIII

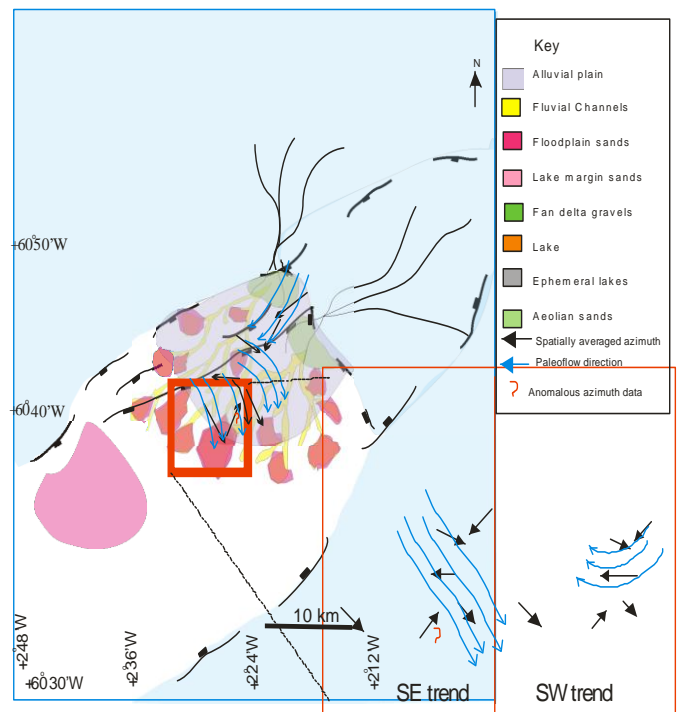


Figure 13: Paleoflow for unit VII/VIII plotted on the paleogeographic map showing an additional northern source (after Allen & Mange-Rajetzky, 1992).

Heavy mineral assemblages as established by Schmidt et al, (2013), Allen & Mange-Rajetzky, (1992) and Morton (2012) include: dominant type 2 zircon, dominant GZi, high SZi and RuZi, low ATi, staurolite, high Unstables : Tourmaline (UTi) and Chloritoid (Figure 12). The paleogeographic model by Allen & Mange-Rajetzky, (1992) suggests sediment input from the NE of the basin possibly as a result of uplift in the NE (Figure 13).

The derived palaeocurrent indicates sourcing from the north and NE of the basin. Confirming the change in provenance is an increase in GZi, decreasing ATi and a type 2 zircon different from those found in the underlying units because it indicates provenance from a moderate to high staurolite and garnet rich metasedimentary rock which could possibly be sourced from East Greenland, Scandinavia or Scotland (schmidt et al, 2013; Allen & Mange-Rajetzky, 1992). The SW palaeocurrent implies sourcing from East Greenland or Scandinavia. The high sinuosity of the SW trend

indicates a meandering river implying potential point bars downstream towards the centre of the basin (Figure 14).

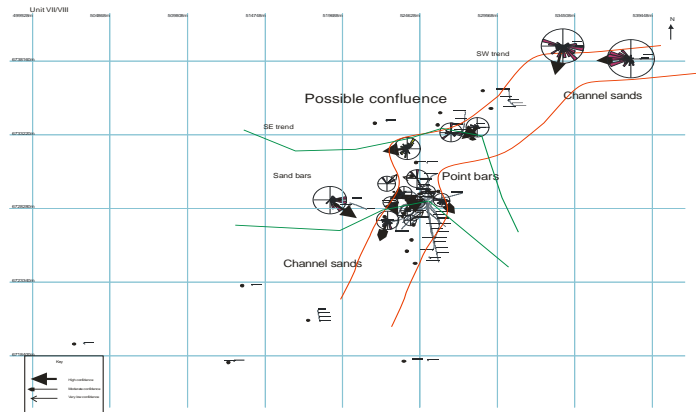


Figure 14: Base map showing the interpreted river course and the potential sandstone distribution for Unit VII/VIII.

Unit IX

Unit IX consists of sandstone. The rose diagram features a dominant SW trend with scatter in the WNW direction (Figure 15). The regional scale shows a dominant SW and a minor SE azimuthal trend. Both are unidirectional NE of the basin and scatters downstream. The sinuosity index is low up stream, increases towards the cluster and then reduces downstream. On a local scale, the predominant NW trend is unidirectional accompanied with high sinuosity that decreases downstream. While the NE trend is dominant within the cluster but scatters downstream accompanied with a low sinuosity across the cluster (Appendix 22).

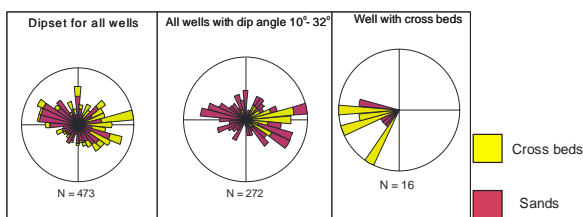


Figure 15 Paleotransport analysis result from interpreted lithofacies dip set for Unit IX.

Heavy mineral assemblages as established by (Morton & Milne, 2012 ; Schmidt *et al.*, 2013) consists of type 2 zircon, high GZi, RuZi, SZi, low ATi and UTi (Figure 16). Nichols, 2005 paleogeographic model suggests provenance from the southern and northeastern part of the basin.

Dispersal pattern indicates the north and NE as major sources with the south as a minor source. These transverse rivers reflect structural control. Consistent with the dispersal pattern is the type 2 zircon with East Greenland, Scandinavia and Scotland as likely sources and the paleogeography (Allen & Mange-Rajetzky, 1992) suggesting provenance from the S and NE. The high sinuosity values of the NW and SW palaeocurrent reflect meandering rivers with implications for point bars upstream (Figure 17).

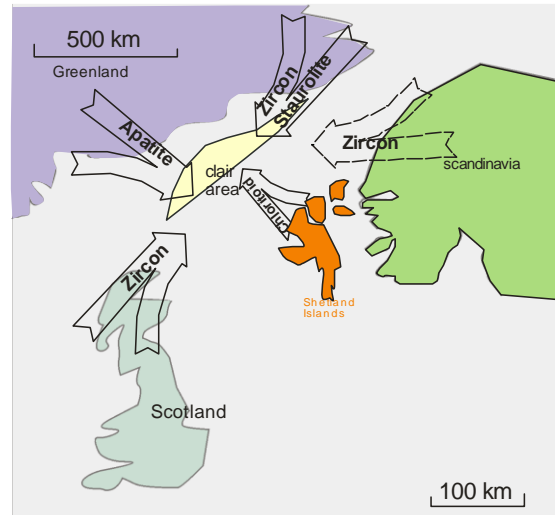


Figure 16: Provenance map Showing a variety of sources derived from heavy mineral assemblage. probable sources in bold lines and less likely sources in dashed lines showing an increase in drainage area (after Morton & Milne, 2012).

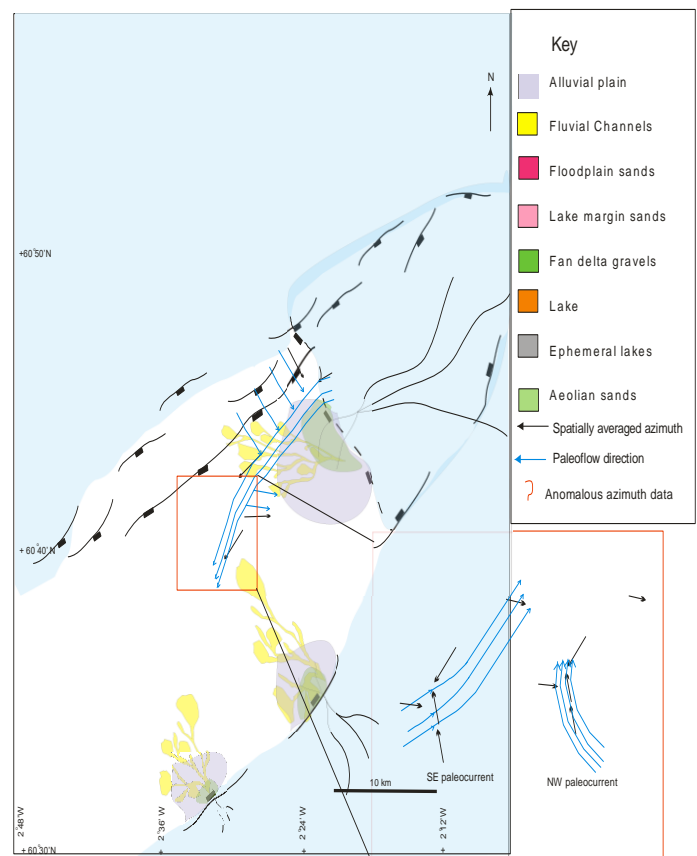


Figure 17: paleoflow for unit IX plotted on the paleogeographic map (Allen & Mange-Rajetzky, 1992).

V. CONCLUSION

The Clair Field, the largest offshore oil and gas accumulation in the UK Continental Shelf (UKCS), holds vast hydrocarbon reserves. However, its complex geological history presents significant challenges for hydrocarbon recovery, primarily due to reservoir compartmentalization and

heterogeneity, driven by an intricate network of faults and fractures. This study advances understanding of the provenance and paleotransport dynamics of Carboniferous sandstones in the Clair Field, revealing a complex interplay of tectonic activity, climatic shifts, and sediment dispersal processes. The findings demonstrate that the transition from humid to arid conditions, coupled with a shift from high- to low-sinuosity fluvial systems, has played a critical role in shaping reservoir quality and connectivity. These results underscore the importance of integrating paleotransport analysis with heavy mineral and paleogeographic data to refine sedimentary models and their implications for reservoir architecture. By enhancing predictive models of reservoir distribution and quality, this research provides valuable insights for hydrocarbon exploration and production in the Clair Field and other structurally complex sedimentary basins.

VI. RECOMMENDATION

It is recommended that Advanced reservoir modelling techniques, including 3D seismic interpretation, dynamic modelling and reservoir simulation, should be employed to identify hydrocarbon pools, better predict fluid flow and optimize production strategies. In addition, given the evidence of southern sediment sources in Units III and Lower Unit VI, further exploration should focus on the southern parts of the basin to identify additional hydrocarbon reserves.

REFERENCES

1. Aitken, J.F. & Howell, J.A. 1996, "High resolution sequence stratigraphy: innovations, applications and future prospects", *Geological Society, London, Special Publications*, vol. 104, no. 1, pp. 1-9
2. Allen, P. A., & Allen, J. R. (2005). Basin analysis: Principles and application to petroleum play assessment. Wiley-Blackwell.
3. Allen, P. A., & Mange-Rajetzky, M. A. (1992). Devonian-Carboniferous sedimentary evolution of the Clair Area, offshore north-western UK: impact of changing provenance. *Marine and Petroleum Geology*, 9(1), 29-52
4. BALCKBOURN, G. (1987). Sedimentary environments and stratigraphy of the Late Devonian-Early Carboniferous Clair basin, west of Shetland. *Geological journal. Special issue*, (12), 75-91
5. Bilal, A., Xie, Q., & Zhai, Y. (2020). Flow, sediment, and morphodynamics of river confluence in tidal and non-tidal environments. *Journal of Marine Science and Engineering*, 8(8), 591.
6. Boggs, S. (2011). *Principles of Sedimentology and Stratigraphy*. Pearson Education.
7. BP. (2021). Clair Field: Overview and Development. Retrieved from https://www.bp.com
8. Castle, J.W. (2001). Appalachian basin stratigraphic response to convergent-margin structural evolution. *Geological Society of America Bulletin*, 113(1), 83-103.
9. Coney, D., Fyfe, T. B., & Price, J. D. (1993). The Clair Field: A major hydrocarbon accumulation in the West of Shetland Basin. *Petroleum Geoscience**, 1(1), 43-52
10. Dean, K., et al. (2015). The geological evolution of the West of Shetland Basin. Geological Society, London, Petroleum Geology Conference Series, 8, 131-144
11. Dickinson, W.R. 1988, "Provenance and sediment dispersal in relation to paleotectonics and paleogeography of sedimentary basins" in *New perspectives in basin analysis* Springer, pp. 3-25
12. Dickinson, W.R., & Gehrels, G.E. (2009). Use of detrital zircon ages in sedimentary provenance studies. *Sedimentary Geology*, 217(1-4), 147-161.
13. Fletcher R., Kuszniir N., Roberts A. & Hunsdale R. 2013. The formation of a failed continental breakup basin: The Cenozoic development of the Faroe-Shetland Basin. *Basin Research*, 25, 532-553.
14. Glennie, K. W. (2010). *Desert sedimentary environments*. Elsevier.
15. Ghosh, K. G. (2022). Sediment transport at the river confluences: few observations from a sub-tropical plateau fringe river of eastern India. *Geology, Ecology, and Landscapes*, 6(2), 75-98.
16. Groshong, R.H. (1999). 3D Structural Geology. *Springer*
17. Hartley, A., et al. (2013). Fluvial systems in rift basins: sediment dispersal in extensional settings. *Sedimentary Geology*, 289, 1-16.
18. Harvey, A. M. (2002). The role of alluvial fans in the geological and geomorphological evolution of mountainous regions. *Zeitschrift für Geomorphologie*, 127, 1-19.
19. Johnson, H. D., et al. (2015a). Stratigraphy and sedimentology of the Clair Field, West of Shetland. Geological Society, London, Petroleum Geology Conference Series, 8, 145-158
20. Johnston, S.C., Smith, R.I. & Underhill, J.R. 1995a, "The Clair Discovery, west of the Shetland Isles", *Scottish Journal of Geology*, vol. 31, no. 2, pp. 187-190.
21. Johnston, S.C., Smith, R.I. & Underhill, J.R. 1995b, "The Clair Discovery, west of the Shetland Isles", *Scottish Journal of Geology*, vol. 31, no. 2, pp. 187-190.
22. Kleinhans, M.G., Cohen, K.M., Hoekstra, J. & IJmker, J.M. 2011, "Evolution of a bifurcation in a meandering river with adjustable channel widths, Rhine delta apex, The Netherlands", *Earth Surface Processes and Landforms*, vol. 36, no. 15, pp. 2011-2027.
23. Lovell, M.A., Williamson, G., & Harvey, P.K. (1999). Borehole Imaging: Applications and Case Histories. *AAPG Memoir 61*.
24. McKie, T. & Garden, I. 1996, "Hierarchical stratigraphic cycles in the non-marine Clair Group (Devonian) UKCS", *Geological Society, London, Special Publications*, vol. 104, no. 1, pp. 139-157.
25. Morton, A., Hallsworth, C., Kunka, J., Laws, E., Payne, S., & Walder, D. (2010). Heavy-mineral stratigraphy of the Clair Group (Devonian-Carboniferous) in the Clair Field, West of Shetland, UK.
26. Morton, A., & Milne, A. (2012). Heavy mineral stratigraphic analysis on the Clair Field, UK, west of Shetlands: a unique real-time solution for red-bed correlation while drilling. *Petroleum Geoscience*, 18(1), 115-128.
27. Munns, J. W., et al. (2015). Reservoir geology of the Clair Field, West of Shetland. Geological Society, London, Petroleum Geology Conference Series, 8, 159-172.
28. Nichols, G. J. (2005). Sedimentary evolution of the Lower Clair Group, Devonian, West of Shetland: climate and sediment supply controls on fluvial, aeolian and lacustrine deposition. In *Geological Society, London, Petroleum Geology Conference Series* (Vol. 6, No. 1, pp. 957-967). The Geological Society of London.
29. Nichols, G. 2007; 2009, "Fluvial Systems in Desiccating Endorheic Basins" in *Sedimentary Processes, Environments and Basins* Blackwell Publishing Ltd., , pp. 569-589.
30. Nichols, G.J. & Fisher, J.A. 2007, "Processes, facies and Architecture of fluvial distributary system deposits", *Sedimentary Geology*, vol. 195, no. 1-2, pp. 75-90.
31. North, C.P. & Prosser, D.J. 1993, "Characterization of fluvial and aeolian reservoirs: problems and approaches", *Geological Society, London, Special Publications*, vol. 73, no. 1, pp. 1-6
32. Oil & Gas UK (2020). Clair Field. Oil & Gas UK Website
33. Posamentier, H.W., & Kolla, V. (2003). Seismic geomorphology and stratigraphy of depositional elements in deep-water settings. *Journal of Sedimentary Research*, 73(3), 367-388.
34. Potter, P.E., and Pettijohn, F.J., 1977, Paleocurrent and Basin Analysis, Second. Edition: Springer, 425 p. 283
35. Reineck, H.E., & Singh, I.B. (1980). Depositional Sedimentary Environments. *Springer*.
36. Rider, M. and Kennedy, M. (2011) The Geological Interpretation of Well Logs, 3rd edition, Rider French Consulting Ltd.
37. Ritchie, J. D., Ziska, H., Johnson, H., & Evans, D. (1999). Geological evolution of the West of Shetland Basin: Implications for hydrocarbon exploration. *Geological Society, London, Special Publications**, 164(1), 327-348.
38. Robertson, A. G., & Ball, M. (2020). *The Clair Field, Blocks 206/7a, 206/8, 206/9a, 206/12a and 206/13a, UK Atlantic Margin*.

Geological Society, London, Memoirs, 52, 931–951. (Development history)

39. Schmidt, A. S., Morton, A. C., Nichols, G. J., & Fanning, C. M. (2012). Interplay of proximal and distal sources in Devonian–Carboniferous sandstones of the Clair Basin, west of Shetland, revealed by detrital zircon U–Pb ages. *Journal of the Geological Society*, 169(6), 691-702.

40. Schmidt, A.S., et al. (2013). Interplay of proximal and distal sources in Devonian-Carboniferous of the Clair Basin. *Journal of the Geological Society*, 170(1), 224.

41. Stoker, M. S., et al. (2017). The Mesozoic evolution of the West of Shetland Basin. Geological Society, London, Petroleum Geology Conference Series, 9, 151-164

42. TSK-06-06, 2009 Final well report Task Geosciences.

43. TSK-09-37 2009 Clair fracture study, Task Geoscience.






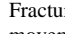
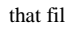


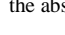
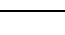
44. Tucker, M.E. (2003). *Sedimentary Rocks in the Field*. Wiley.

45. International Journal of Remote Sensing, vol 31, issue 19, pp 51275143, 2010.

Appendix

Well	Well type	Upper Unit VI	Unit VII/VIII	Unit IX	Unit X
208/08-08	Vertical	169	247		
206/08-9Y	Deviated		48	84	
206/8-A05	Horizontal				
206/8- A15	Deviated	90			
206/8-A03Z	Horizontal	333			
206/8-A02	Vertical				
206/8-15	Vertical	298	299		
X	Horizontal	229	23		
206/08-A13	Horizontal	272			
206/8-A04	Horizontal				
206/8-A11	Deviated	240	233	Not determined	
206/08/13Z	Deviated				
206/08-A 10	Deviated	163	207		
206/08-A 06X	Horizontal	306			
X	Horizontal	186			
X	Horizontal	351			
X	Vertical	230			
X	Horizontal	115			
206/8-2	Vertical	278	225	305	Not determined
206/9-2	Vertical	219	202	126	
206/7-1	Vertical		127		
206/9-1	Vertical		265	267	
206/8-14Z	Deviated				
206/8-A08Z	Deviated	342	314	313	
206/8-A12	Deviated	215	246		
206/8-A07	Horizontal	96			
206/8-A14	Deviated	228			
206/8-14	Deviated		115	221	
206/8-13Y	Vertical				
206/8-12A	Deviated			350	
206/8-3A	Vertical		141	85	Not determined
206/8-A09	Horizontal	Not determined	46	222	

Appendix 1a: Derived azimuth vector mean

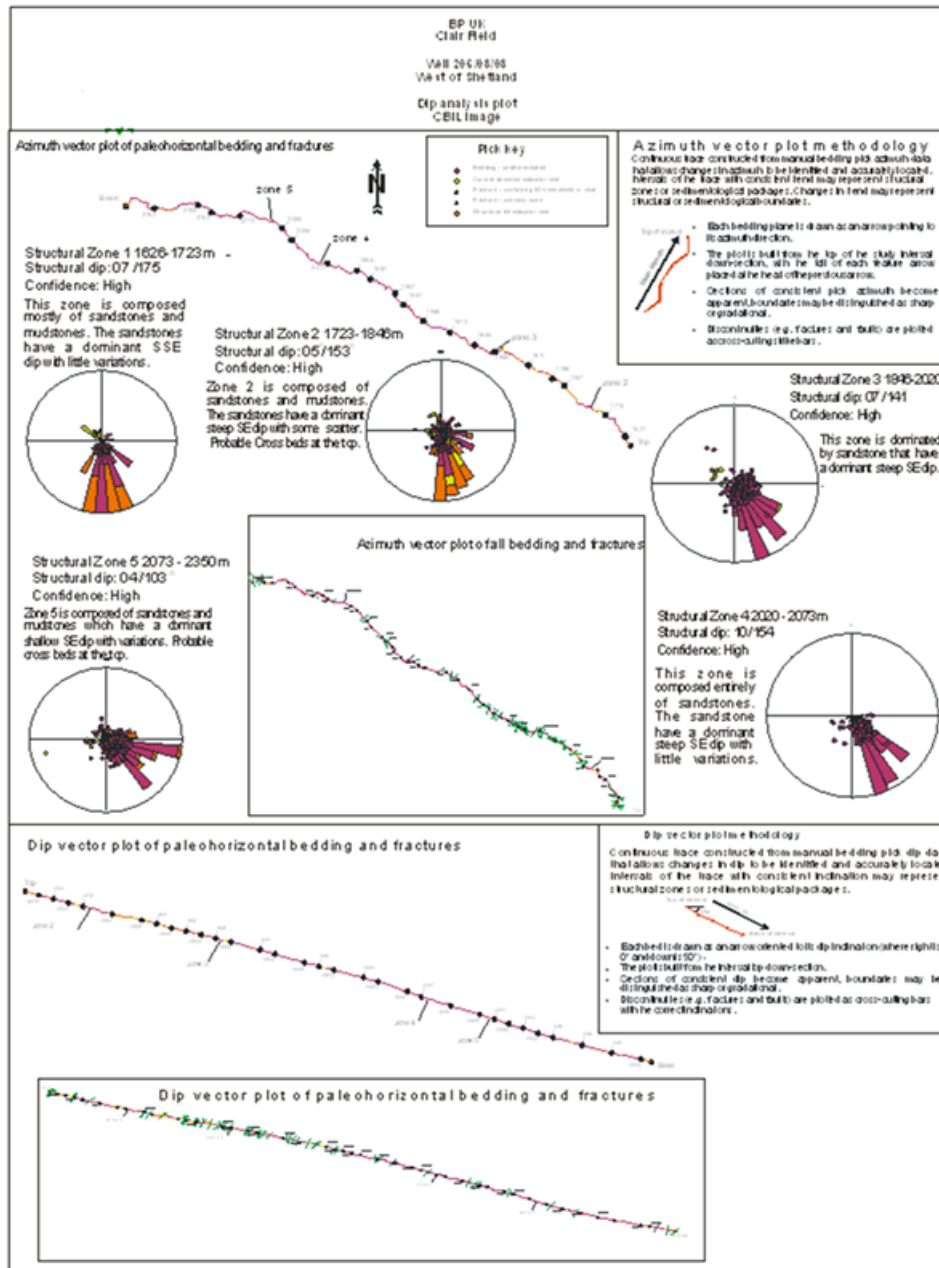
Type	Subtype	Symbol	Description
Faults	Possibly open		Faults indicate that some amount of displacement has occurred along a plane discordant to bedding. The amount of displacement may vary somewhat with the contractor source of data and has not been standardized. Offset cannot generally be quantified.
	Containing fill/mineralised		
	Undifferentiated		
	Brecciated		
Fractures	Possibly open		Fractures are discontinuities across which no (or negligible) displacement has occurred. Cataclasis implies some movement along granulation seams, but significant offset is not recorded. This may be a burial process. Note that fill may not be total and aperture may still be present in this category.
	Partially open/closed		
	Containing fill/mineralised or shut		
	Granulation seams/ cataclastic		
Bedding	Structural tilt indicator		Parallel laminated have been included as a separate category, as they can be used as structural tilt indicators in the absence of mudstonesstones but with lower confidence than mudstonesstone and heterolithic beds.
	Parallel laminated sandstonestone		
	Current direction		

	indicator		
	Undifferentiated	●	

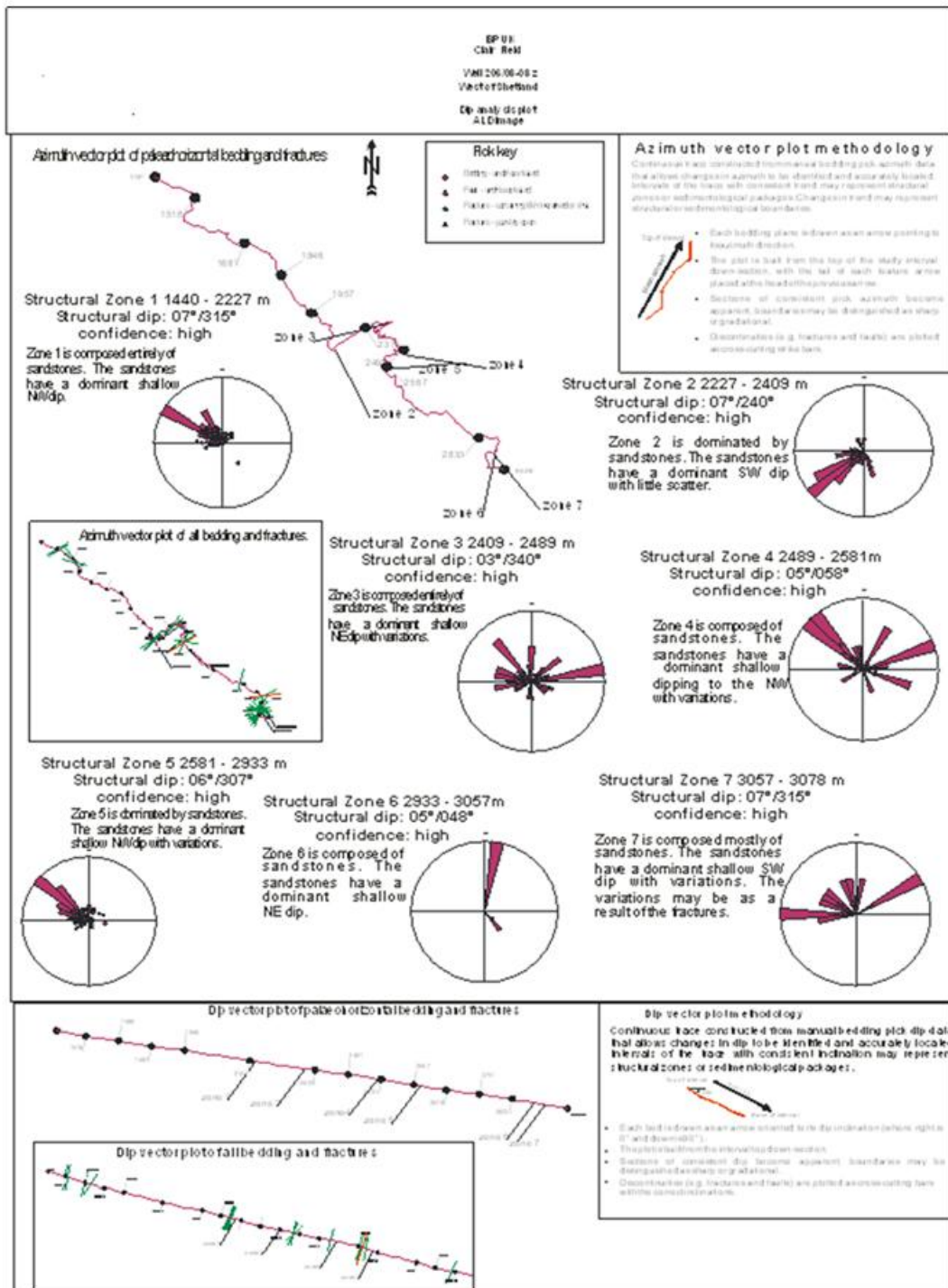
Appendix 1b: Manual dip classification scheme used in the study

Well	UPPER VI		UNIT VI/VII		UNIT IX	
	Measure 1	Measure 2	Measure 1	Measure 2	Measure 1	Measure 2
208/08-08	1.48	1.81	2.58	24.96		
206/08-9Y			1.03	1.03	1.09	1.12
206/8-A05						
206/8-A15	1.11	1.14				
206/8-A03Z	12.434	-1.34				
206/8-A02						
206/8-15	5.04	-2.51	5.14	-2.45		
206/08-A13	3.4	-6.9				
X	2.19	5.71	1.007	1.008		
206/8-A04						
206/8-A11	2.41	10.67	2.27	6.85		
206/08/13Z						
206/08-A 10	1.43	1.71	1.85	3.06		
206/08-A 06X	5.88	-2.11				
X	1.62	2.19				
X	39.04	-1.06				
X	2.21	5.96				
X	1.19	1.26				
206/8-2	3.69	-4.62	2.12	4.91	5.76	-2.15
206/9-2	2.02	4.07	1.79	2.79	1.23	1.33
206/7-1			1.23	1.34		
206/9-1			3.13	-9.52	3.21	-8.21
206/8-14Z						
206/8-A08Z	10.07	-1.19	7.01	-1.81	6.85	-1.84
206/8-A12	1.96	3.66	2.56	20.91		
206/8-A07	1.12	1.17				
206/8-A14	2.17	5.49				
206/8-14			1.19	1.26	2.05	4.31
206/8-13Y			1.3	1.45		
206/8-12A					35	-1.07
206/8-3A			1.3	1.4	1.09	1.12
206/8-A09					2.07	4.45

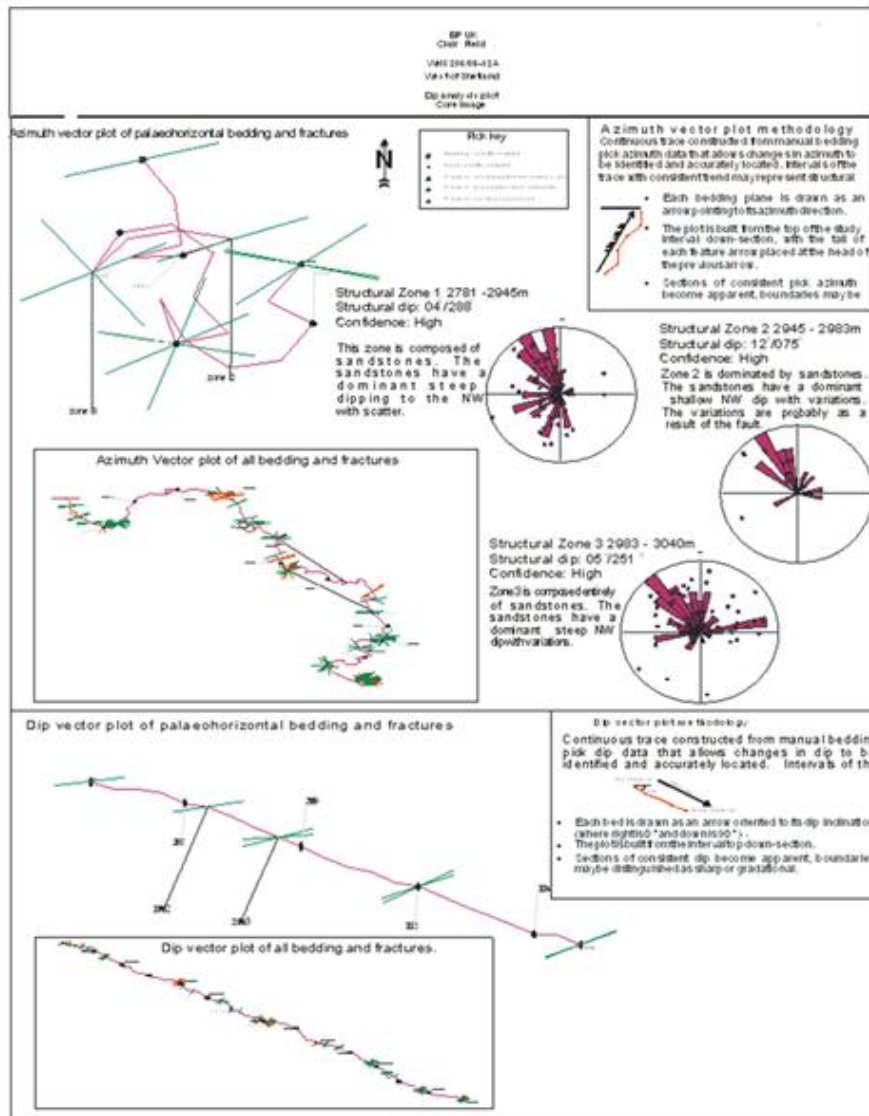
Appendix 2: Sinuosity values



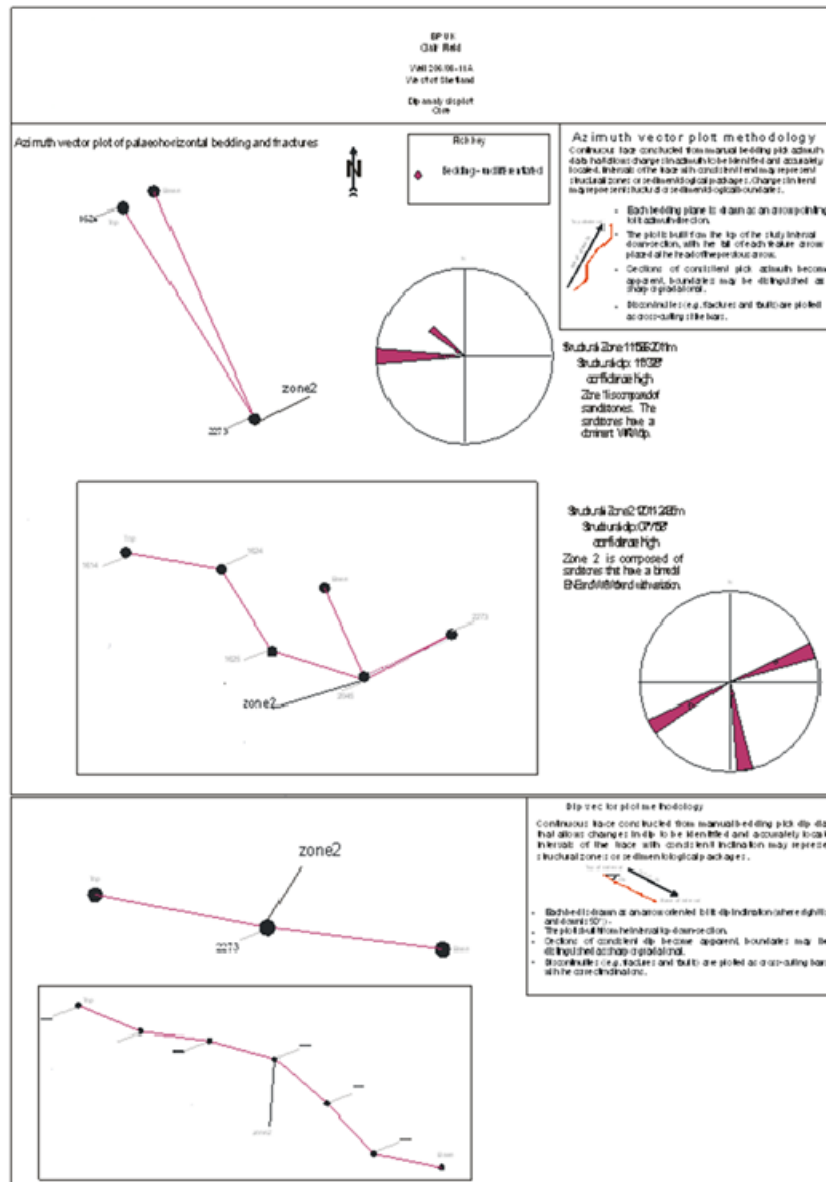
Appendix 3: Dip analysis plot for well 206/08-08



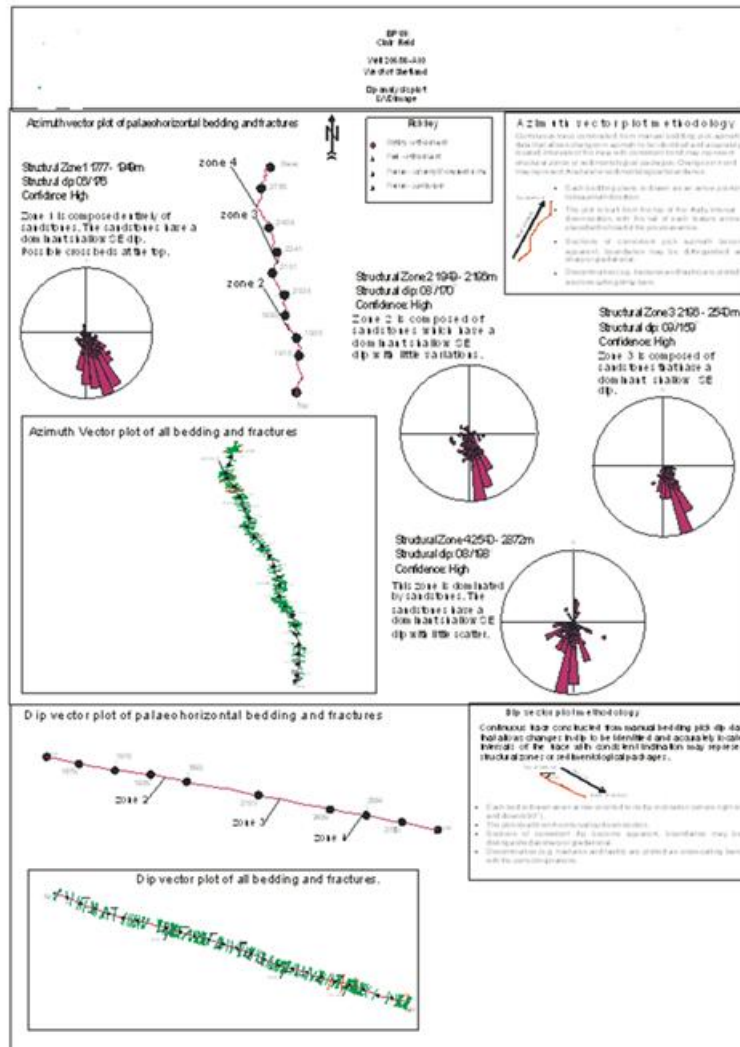
Appendix 4: Dip analysis plot for well 206/08-08Z



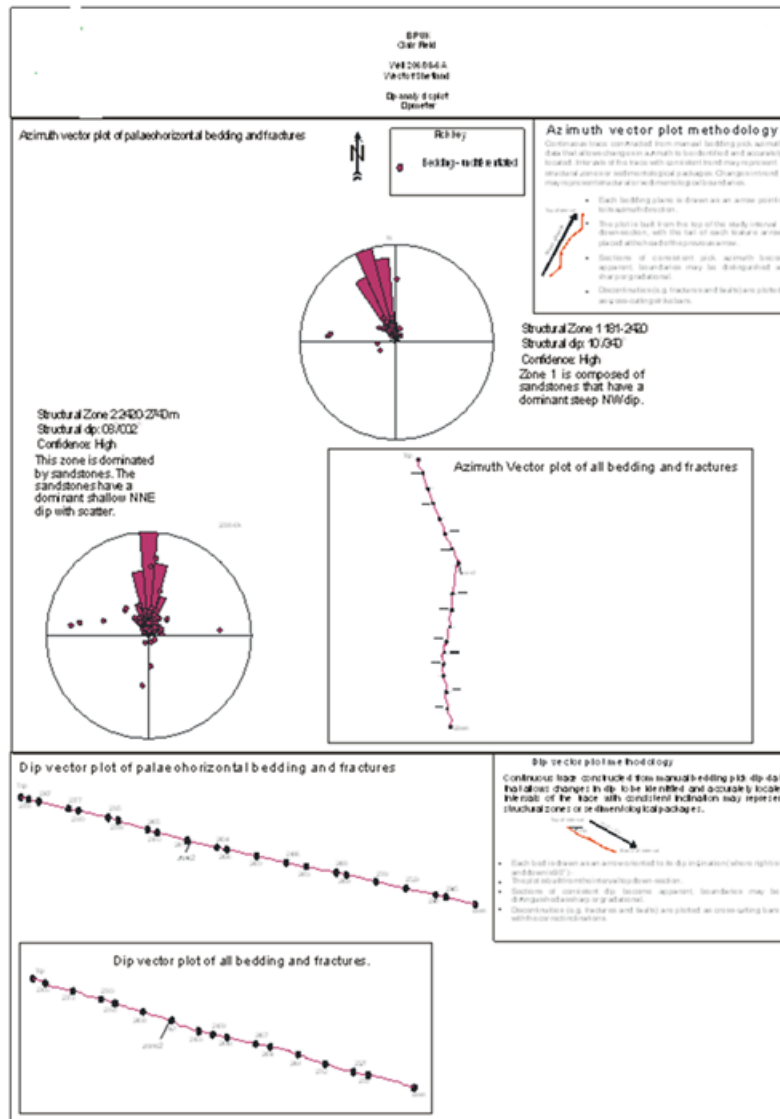
Appendix 5: Dip analysis plot for well 206/08-12A



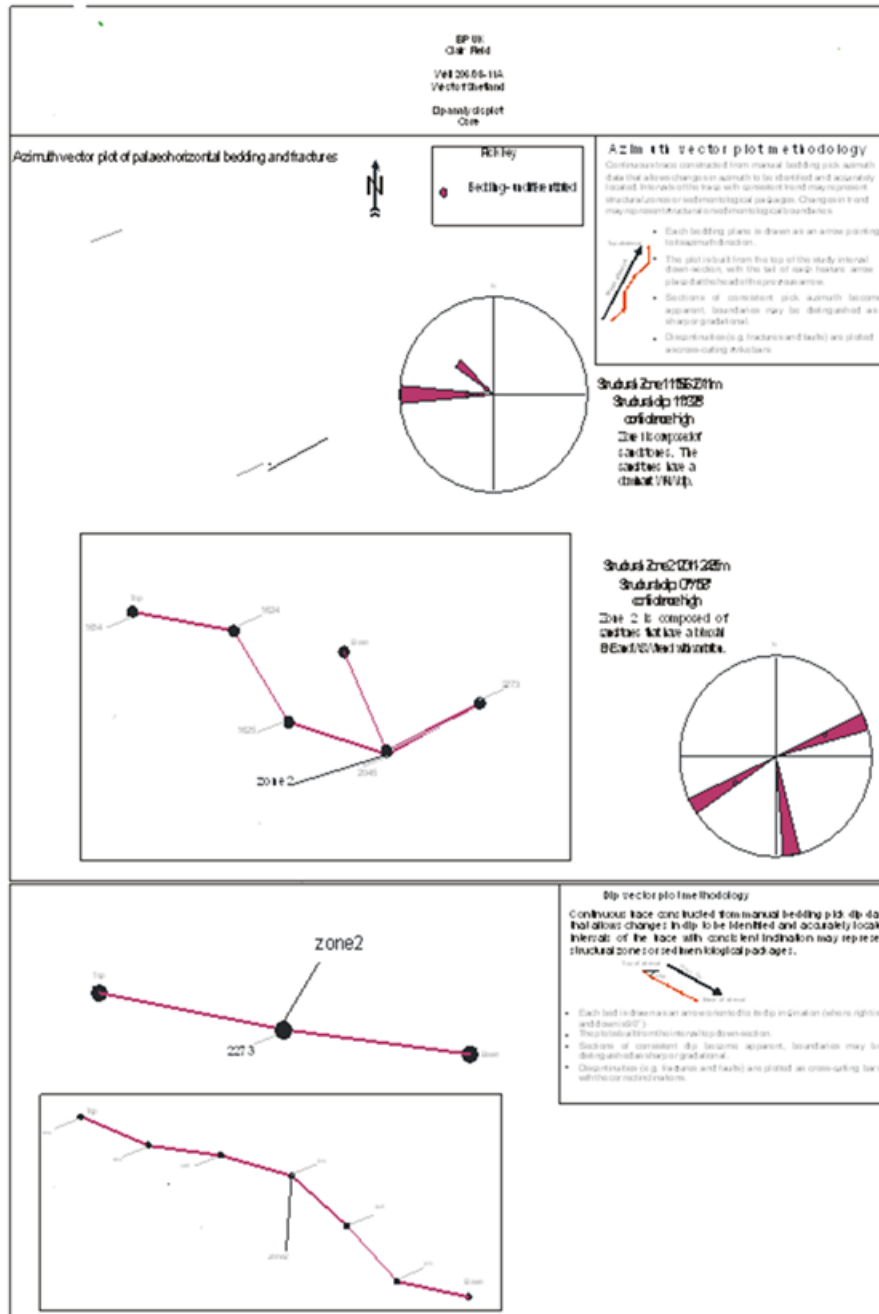
Appendix 6: Dip analysis plot for well 206/08-A11



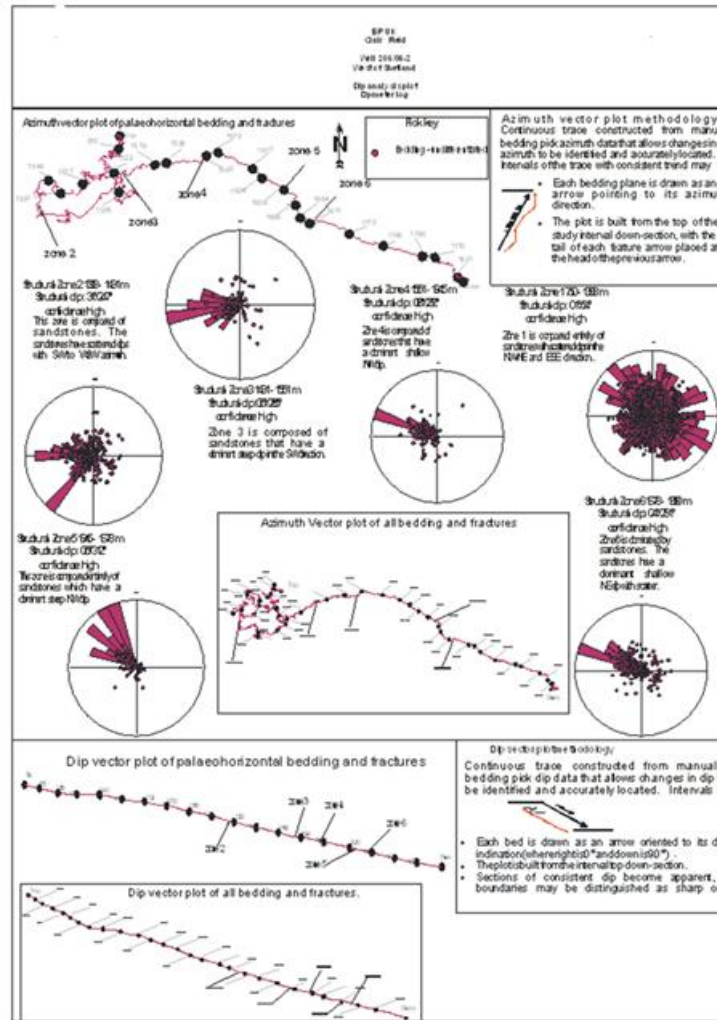
Appendix 7: Dip analysis plot for well 206/08-A10



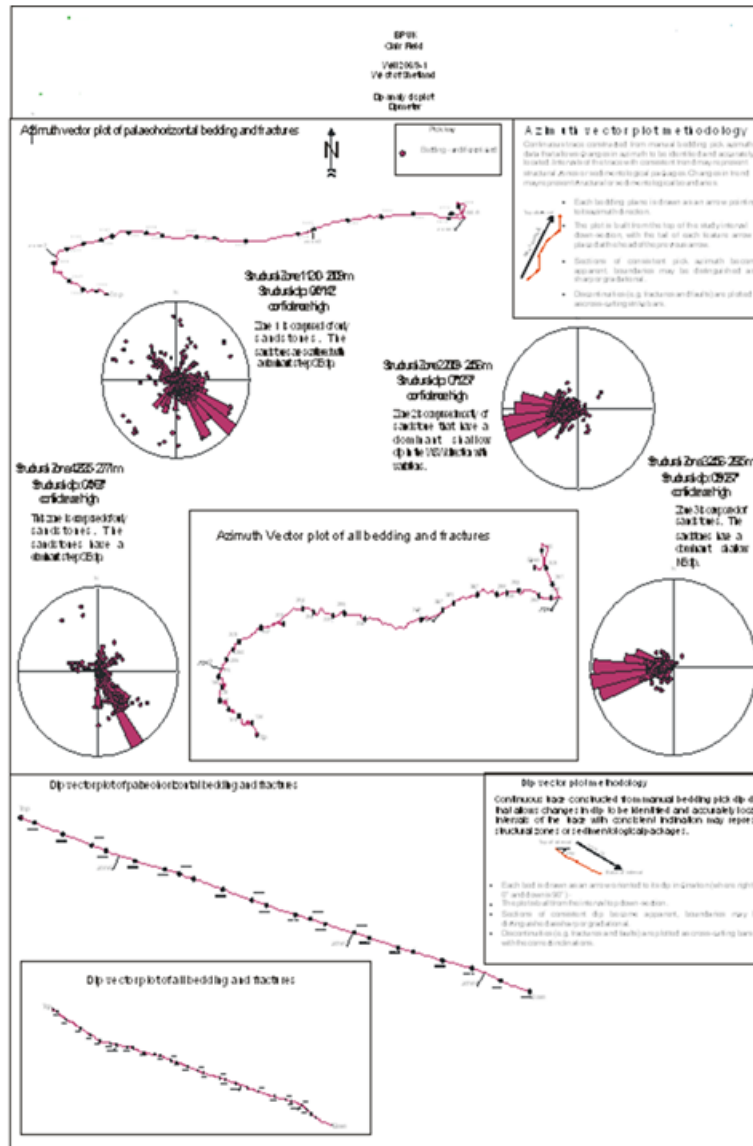
Appendix 8: Dip analysis plot for well 206/08-6A



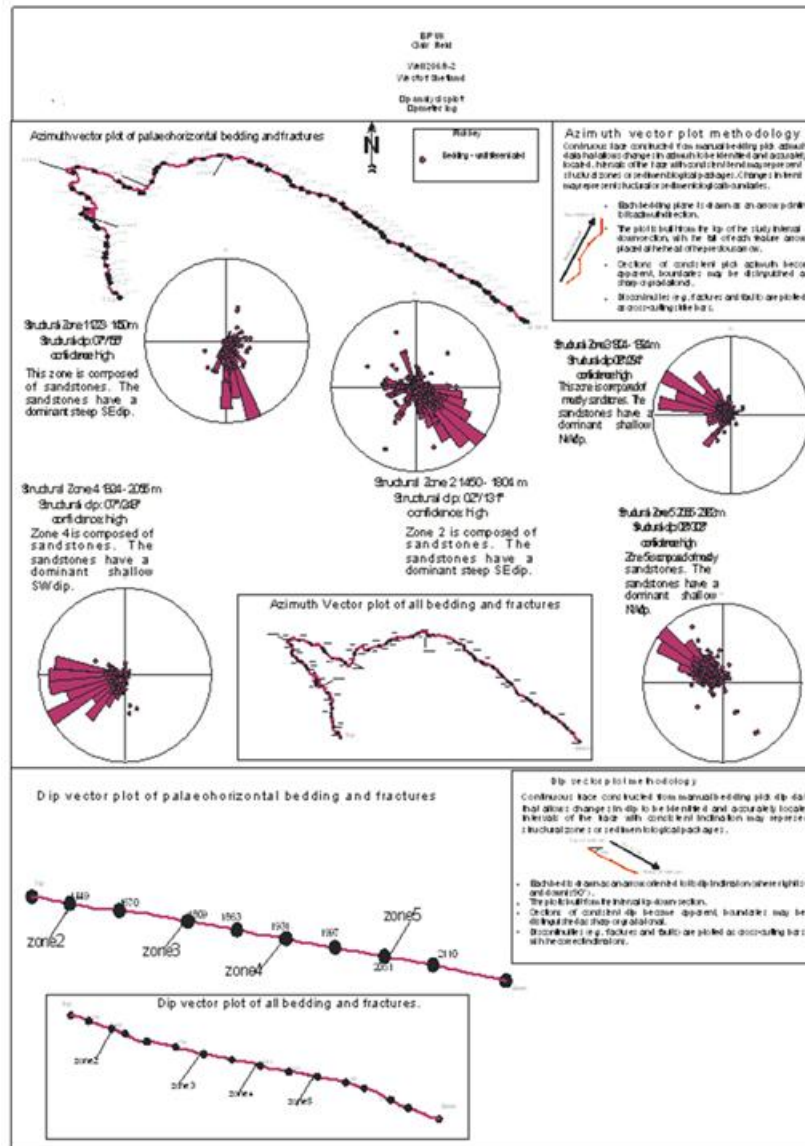
Appendix 9: Dip analysis plot for well 206/08-11A



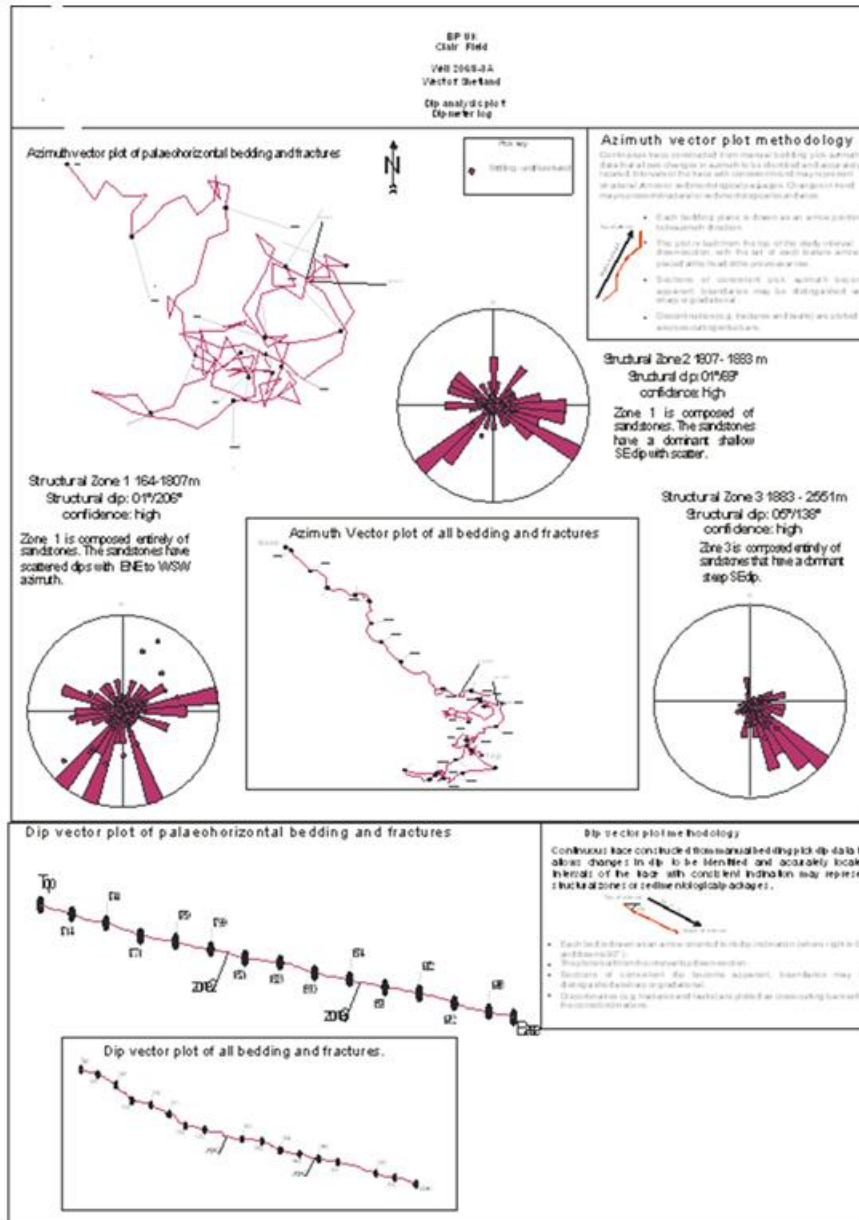
Appendix 10: Dip analysis plot for well 206/8-2.



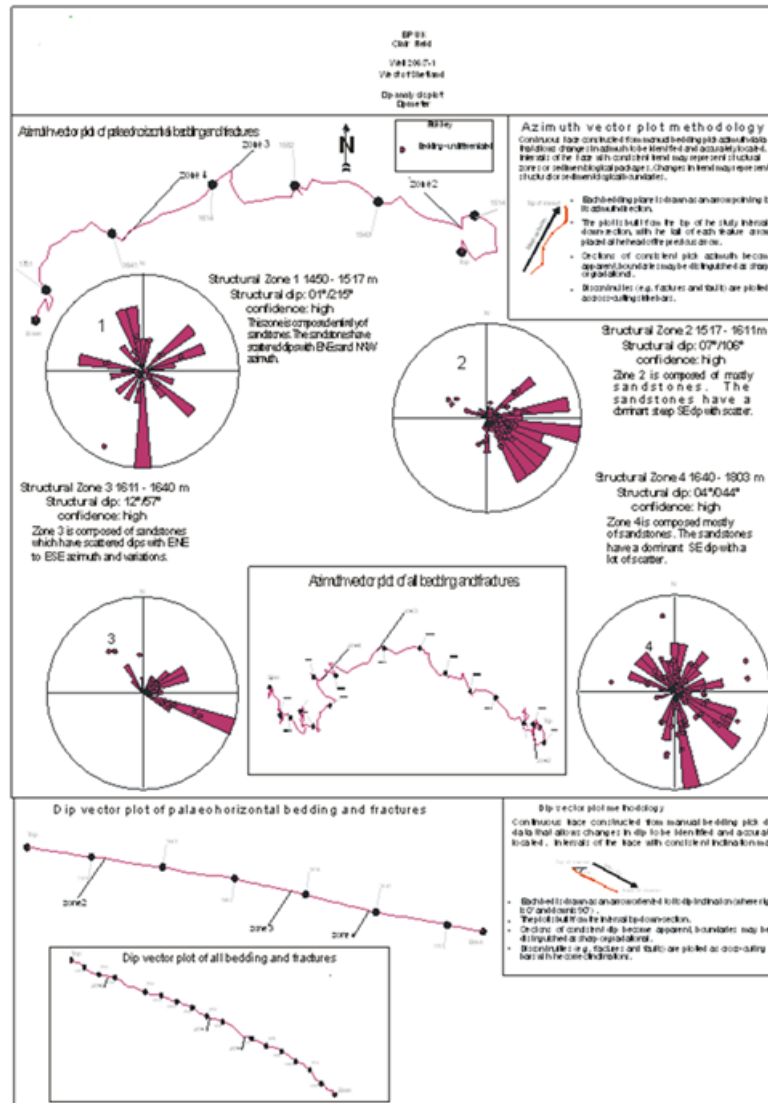
Appendix 11: Dip analysis plot for well 206/9-1.



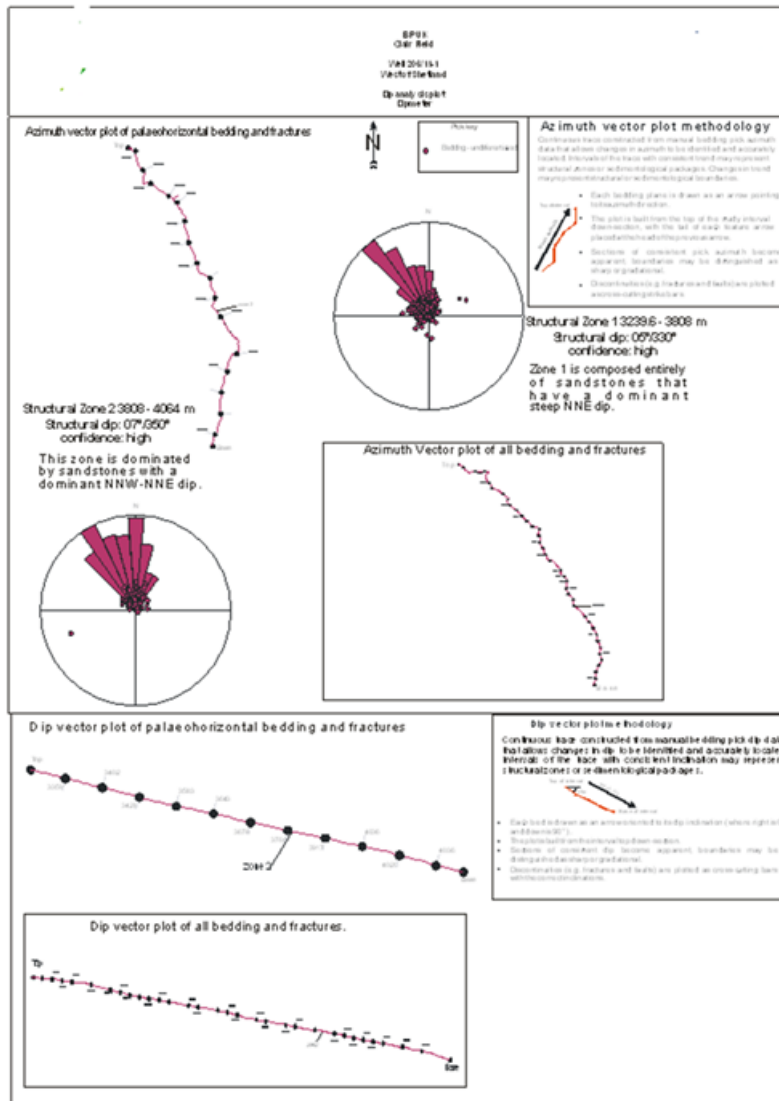
Appendix 12: Dip analysis plot for well 206/9-2.



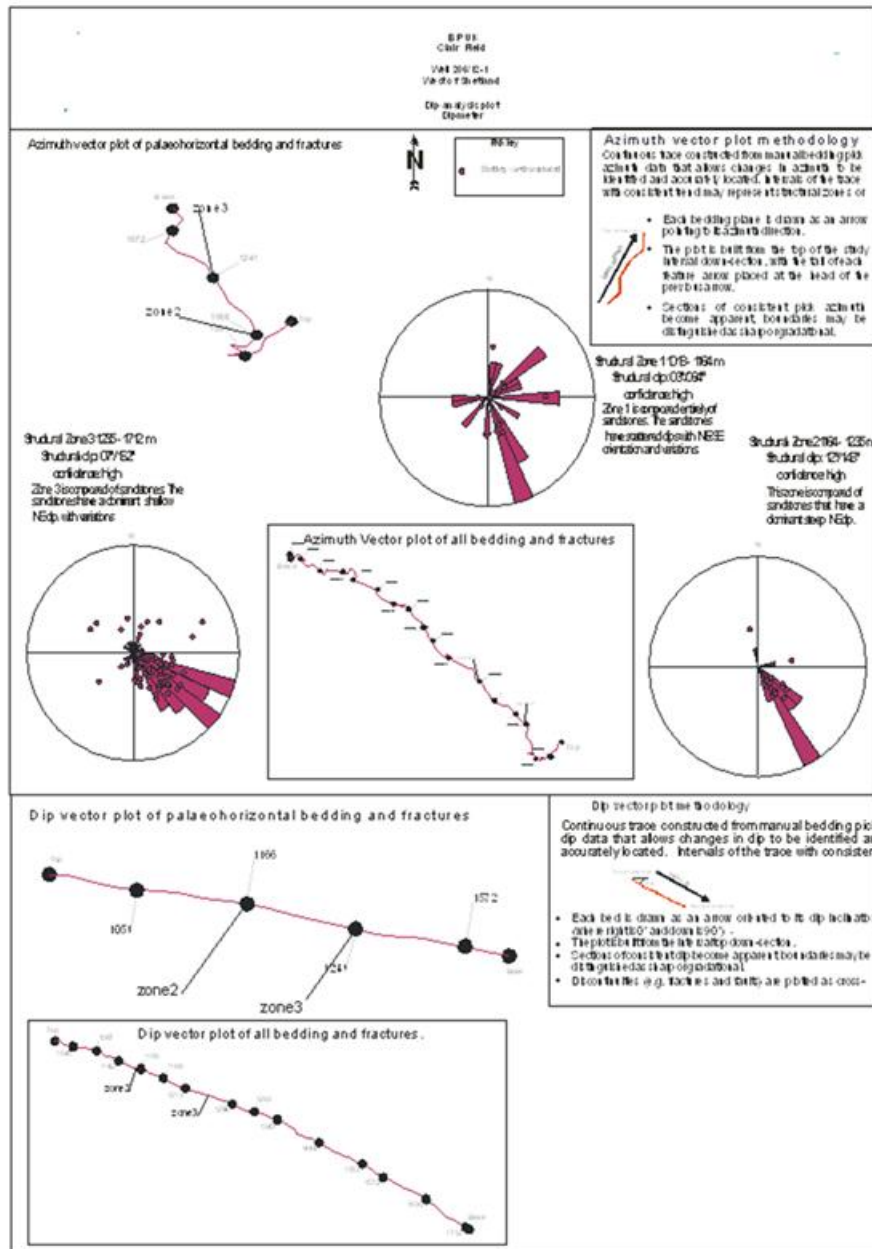
Appendix 13: Dip analysis plot for well 206/08-3A.



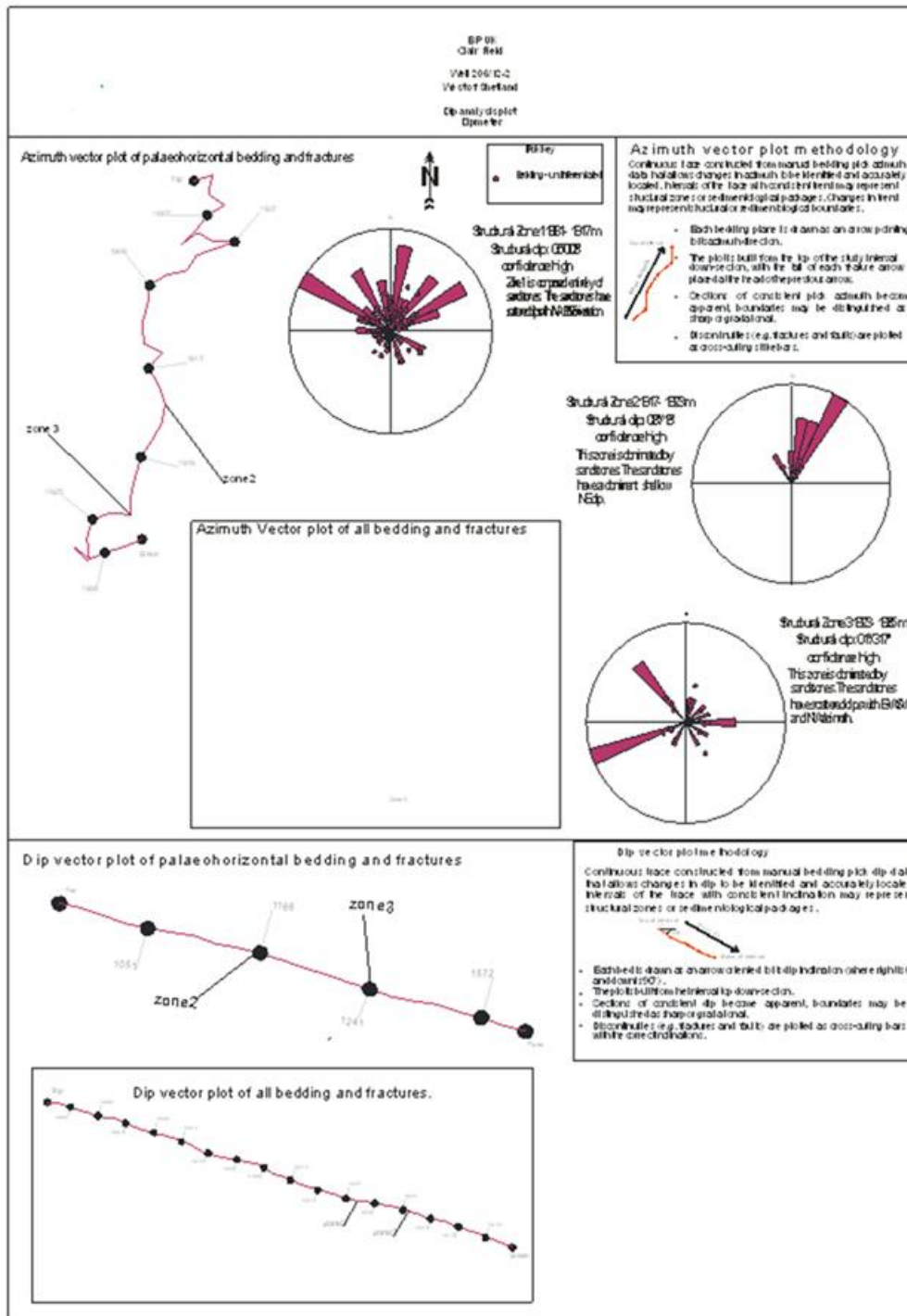
Appendix 14: Dip analysis plot for well 206/7-1.



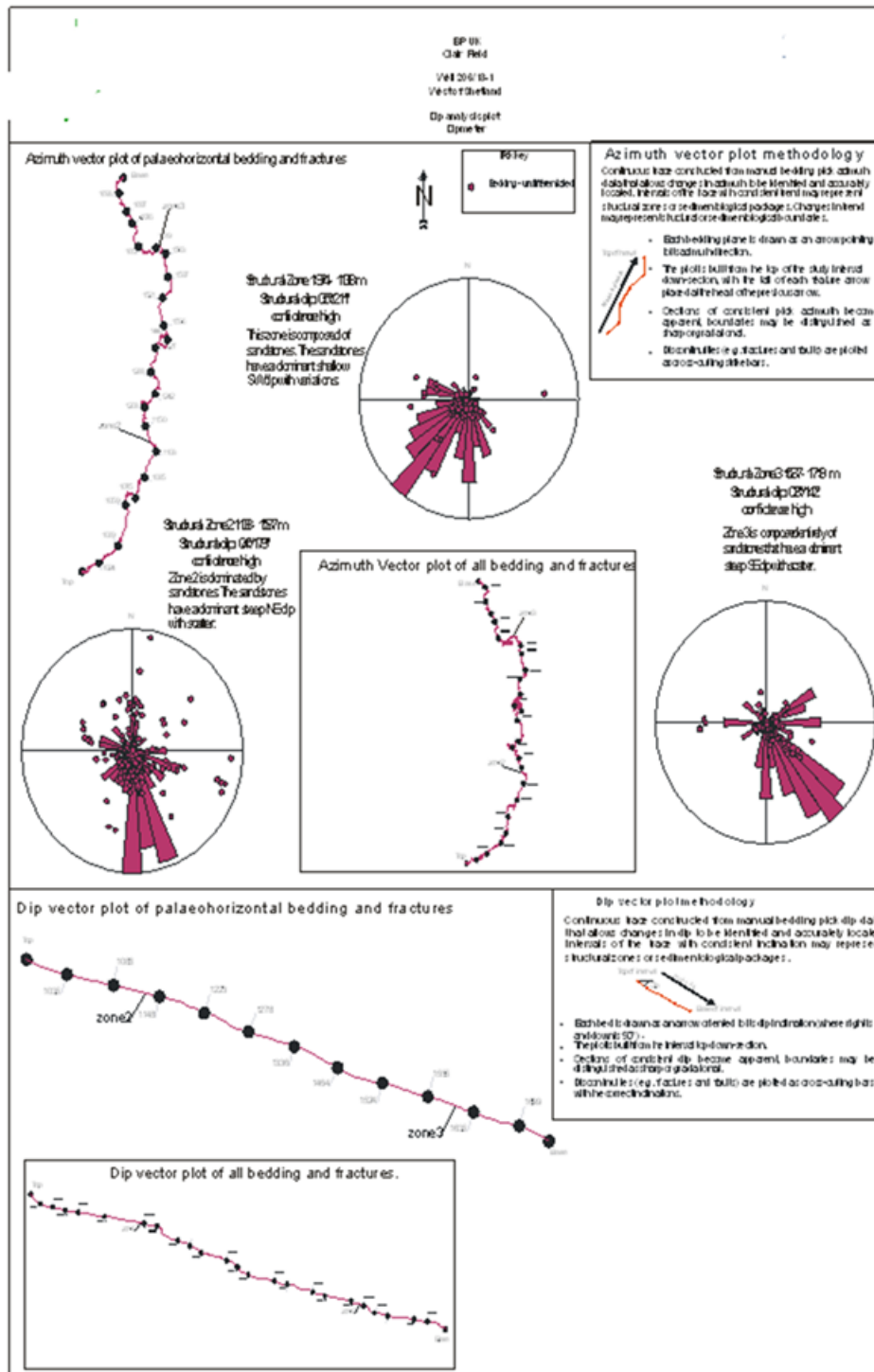
Appendix 15: Dip analysis plot for well 206/11-1.



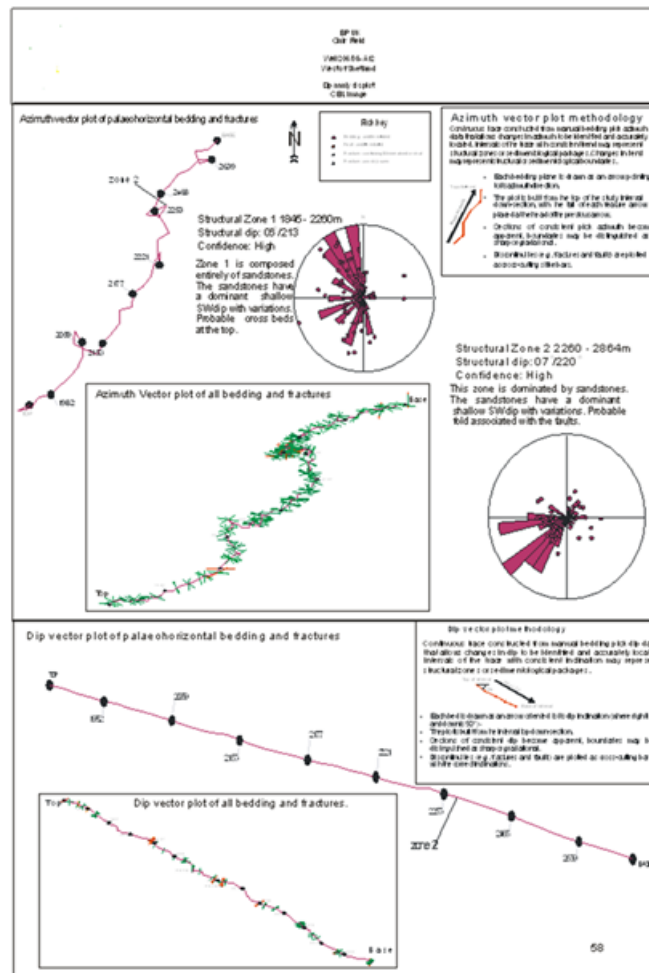
Appendix 16: Dip analysis plot for well 206/12-1.



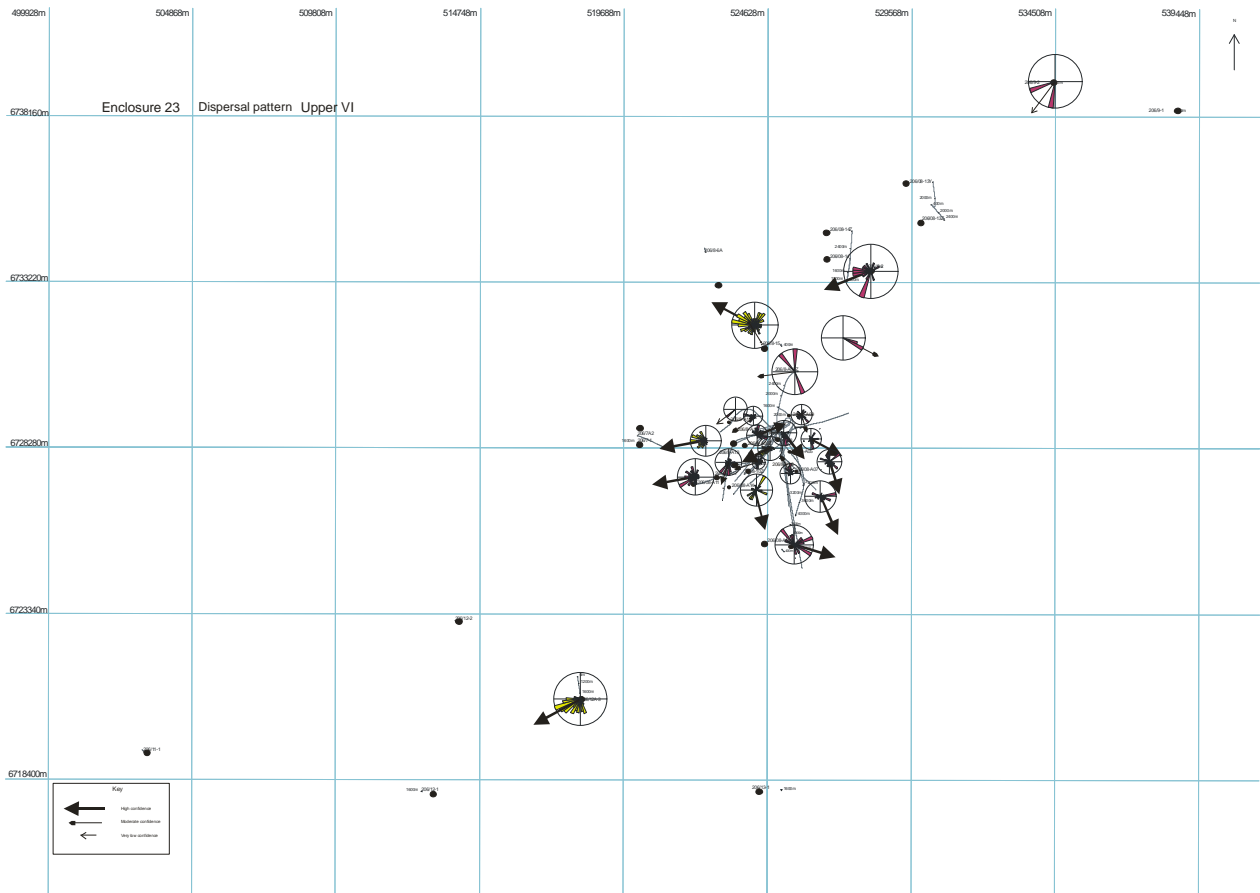
Appendix 17: Dip analysis plot for well 206/12-2



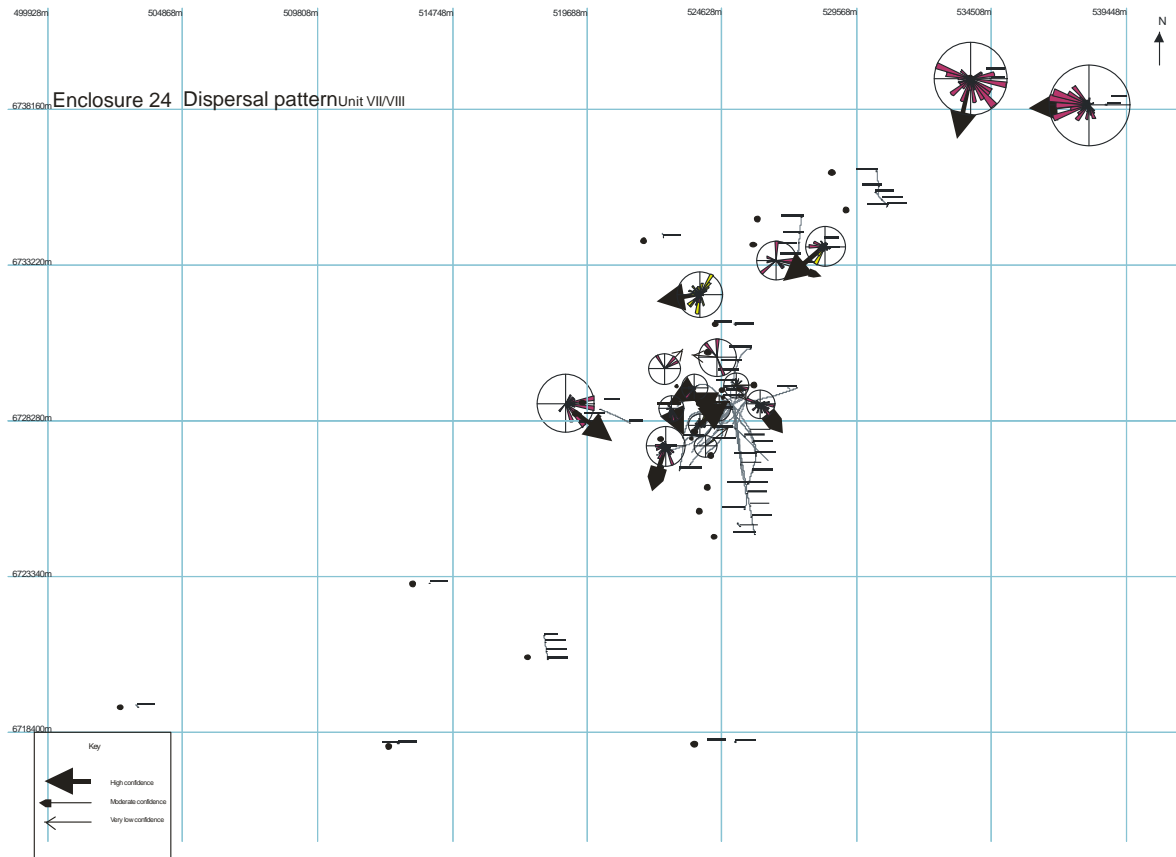
Appendix 18: Dip analysis plot for well 206/13-1



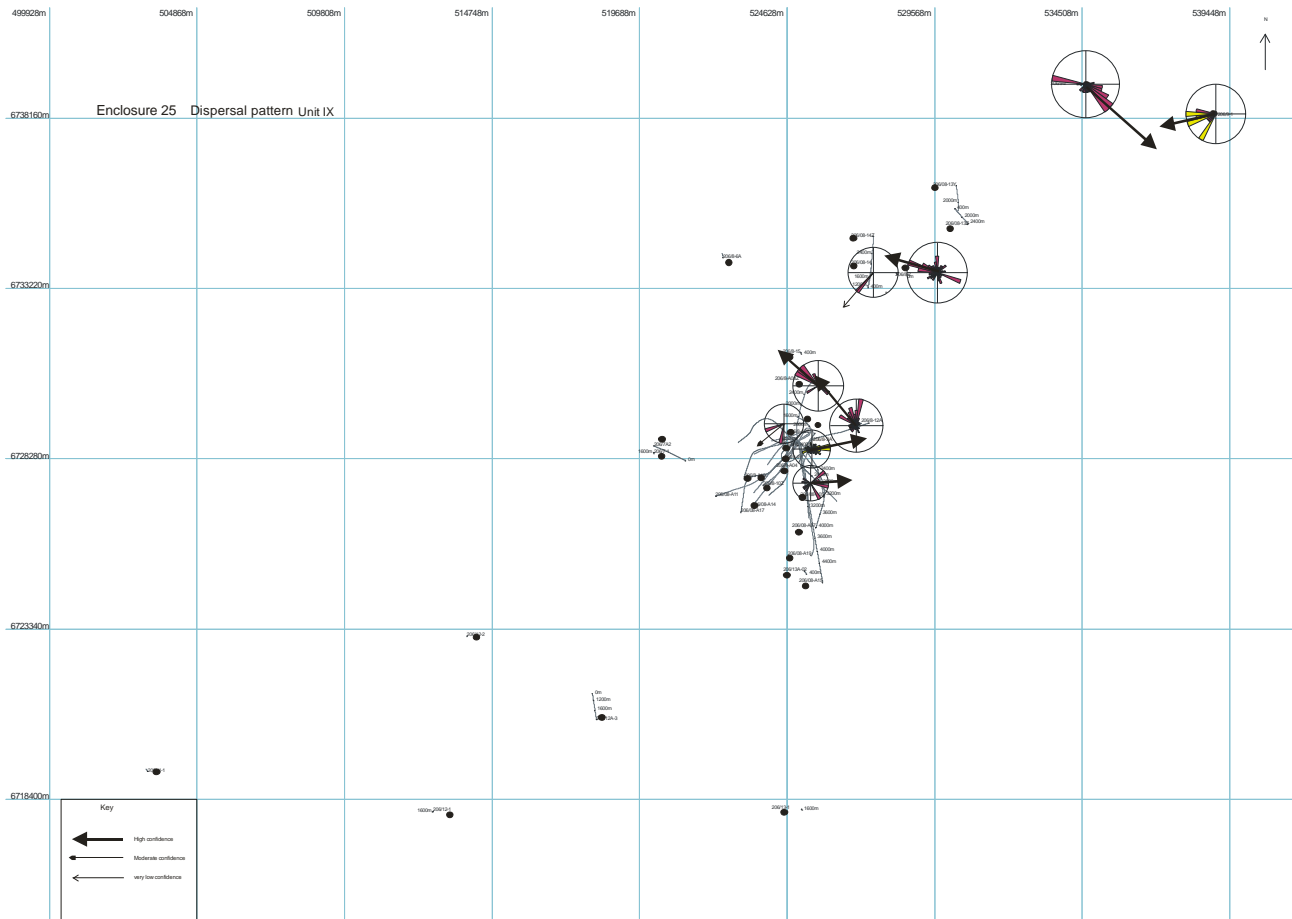
Appendix 19: Dip analysis plot for well 206/08-A12



Appendix 20: Dispersal pattern for Upper Unit VI



Appendix 21: Dispersal pattern for Unit VII/VIII



Appendix 22: Dispersal pattern for Unit IX